RM No. A9D20

NACA

RESEARCH MEMORANDUM

INVESTIGATION OF DOWNWASH AND WAKE CHARACTERISTICS AT A MACH NUMBER OF 1.53

II - TRIANGULAR WING

By Edward W. Perkins and Thomas N. Canning

Ames Aeronautical Laboratory
Moffett Field, Calif.

NATIONAL ADVISORY COMMITTEE
FOR AERONAUTICS

WASHINGTON
June 6, 1949

NACA RM No. A9D20 [redacted]

NATIONAL ADVISORY COMMITTEE FOR AERONAUTICS

RESEARCH MEMORANDUM

INVESTIGATION OF DOWNWASH AND WAKE CHARACTERISTICS AT A MACH NUMBER OF 1.53.

II – TRIANGULAR WING

By Edward W. Perkins and Thomas N. Canning

SUMMARY

The results of an experimental investigation of the downwash and wake characteristics behind a triangular plan-form wing in a supersonic stream are presented. The leading-edge sweep angle and aspect ratio were 63° and 2.04, respectively. The wing had a 5-percent-thick, symmetrical, double-wedge airfoil section with maximum thickness at 50-percent chord. The tests were made at a Mach number of 1.53 and a Reynolds number, based on the mean aerodynamic chord, of approximately 2 million. Measurements were made of the variation of downwash angle with angle of attack at several positions within the induced flow field. Additional surveys were made to determine the position and extent of the friction wake. These experimental results were analyzed and compared with the characteristics calculated by means of the linear theory.

Within that part of the induced flow field where the theory predicts downwash for positive angles of attack of the wing, the experimental values of the variation of the downwash angle with angle of attack through zero lift were found to be in good agreement with the theoretical predictions. Within the remainder of the induced flow field, the agreement was only fair.

At angles of attack, appreciably different from zero, the measured downwash angles at the survey points depart markedly from the values predicted by the theory. The reasons for this departure differ in the positive and negative angle-of-attack ranges since the points at which the downwash angles were measured were at a fixed distance above the chord plane of the wing, and the downwash field, at any finite angle of attack, was not symmetric with respect to the extended chord plane. In the positive angle-of-attack range, the departure was primarily the result of the presence of a strong

[redacted]

vortex in the induced flow field which was not predicted by the linear theory. In the negative angle-of-attack range, this departure may be attributed to the fact that the displacement of the vortex sheet from the free-stream direction was not as great as predicted by the theory.

The general characteristics of the friction wake were similar to those observed in subsonic flow. With increasing distance behind the wing, the wake expanded slowly, decreased in intensity, and with the wing at positive angles of attack, moved downward relative to the free-stream direction.

INTRODUCTION

The satisfactory prediction of longitudinal stability and control of aircraft requires a knowledge of the induced flow field behind lifting surfaces. Two of the primary considerations in this regard are the downwash distribution within the induced flow field and the characteristics of the friction wake. Theoretical calculations of the downwash distribution for conventional lifting surfaces at subsonic speeds are generally based on the familiar Prandtl lifting-line theory. The agreement between the experimentally measured downwash and that calculated in accordance with this approach is satisfactory only when the self-induced movement of the trailing vortex sheet and the local effects of the friction wake are considered. In supersonic flow, several methods based on the linearized differential equation of motion of a compressible fluid have been developed for the computation of downwash. As in subsonic flow, experiment must be relied upon to determine the limits of applicability of these theories to the prediction of downwash in real flows.

The present report is the second of an investigation of downwash and wake characteristics for several representative low-aspect-ratio wing plan forms. Part I of this series (reference 1) was concerned with these characteristics for a wing of rectangular plan form. This report discusses the results for a wing of triangular plan form which was chosen because of its suitability at moderate supersonic Mach numbers as either a lifting wing or a canard-type control surface.

[redacted]

SYMBOLS

x,y,z	longitudinal, lateral, and normal coordinates with the origin at the leading-edge apex of the wing and the x axis corresponding to the free-stream direction
c	wing chord length, inches
H	free-stream total pressure, pounds per square inch absolute
$\Delta H'$	difference between the pitot pressure at a point in the wake and the pitot pressure in the free stream, where the pitot pressure is the pressure measured by a pitot tube in either subsonic flow, where this pressure is equal to the local total pressure, or in supersonic flow, where this pressure is equal to the local total pressure for the flow behind a normal shock wave, pounds per square inch absolute
s	wing semispan, inches
α	wing angle of attack, degrees
ϵ	downwash angle measured from the free-stream direction, degrees
ϵ'	difference between the downwash angle at angle of attack and the downwash angle at $\alpha=0$, degrees

APPARATUS AND TESTS

The investigation was performed in the Ames 1- by 3-foot supersonic wind tunnel No. 1. For these tests the tunnel was equipped with a fixed nozzle which gave a test-section Mach number of 1.53. The test Reynolds number based on the mean aerodynamic chord was approximately 2 million. The experimental procedure employed in this investigation was the same as that described in reference 1 which is Part I of this series of reports. Except where specifically noted, all details of model construction and support, instrumentation, and reduction and correction of data are identical to those described in reference 1. The positions of the three downwash-survey stations and the two wake-survey stations, which are shown in figure 1, were the same as those of reference 1 and, for convenience, the same numbering system has been retained.

[redacted]

Model and Support

The semispan model was of triangular plan form with the leading edge swept back 63° giving an aspect ratio of 2.04. The wing had a 5-percent-thick, symmetrical, double-wedge airfoil section with the maximum thickness at 50-percent chord. The leading and trailing edges were finished to approximately 0.001-inch radius, and the surfaces were ground but not polished. The pertinent dimensions of the model and model support system are shown in figure 1. A more detailed description of the support system and a discussion of the precautions taken to minimize the disturbances in the tunnel air stream caused by the boundary-layer plate are given in reference 1. The orientation of the model, the boundary-layer plate, and the survey instruments is shown in figure 2.

Corrections and Precision

The downwash angles measured at survey stations 2 and 4 were corrected by superposition for stream deflections caused by both the support system and the nonuniformity of the free stream. The data for station 3 have not been corrected for these interference effects since no suitable stream calibration was obtained at this station. However, in view of the relative positions of stations 2 and 3, it is believed that at station 3 these interference effects would be only slightly greater than at station 2. Since the corrections at station 2 are small and have little effect on the final results, it is believed that the uncorrected results presented for station 3 are at least qualitatively useful.

The precision of the present results is the same as that of the results presented in Part I (reference 1). Consideration of the possible sources of error has indicated that the experimental values of ϵ' and α are accurate to within ±0.1° and ±0.05°, respectively On this basis the possible error in determining $(d\epsilon/d\alpha)_{\alpha=0}$ is less than ±0.04. The locations of the friction wake boundaries, which have been taken as the point in the stream where $\Delta H'/H = -0.005$, are correct within ±0.06 inch or approximately 1 percent of the root chord of the wing.

THEORETICAL CONSIDERATIONS

The evaluation of the rate of change of downwash angle with angle of attack is divided into two parts: First, the calculation of $d\epsilon/d\alpha$ at $\alpha=0$, and second, based on these results, the

[redacted]

evaluation of the displacement of the vortex sheet and its effect on the downwash field. The tendency of the shed vorticity to roll up into tip vortices and the resultant effects on the downwash field, are neglected in these computations since no theoretical methods are now available for computing these effects in supersonic flow.

Computation of $\left(\frac{d\epsilon}{d\alpha}\right)_{\alpha=0}$

The method used to compute the rate of change of downwash with angle of attack at zero lift is that outlined in reference 2. This method is essentially a superposition process in which a finite triangular wing is formed from a lifting triangle of infinite chord by cancellation of the lift behind the line which is to be the trailing edge. Thus, the solution may be conveniently divided into two parts: First, the contribution of the lifting triangle of infinite chord to the downwash, and second, the contribution of the constant-load sectors used to form the trailing edge. The general procedure is to start with the solution for a lifting triangle of infinite chord having the same sweep angle of the leading edge as the wing under investigation. This solution is conical with respect to the leading apex. Charts of the downwash field for a series of such lifting surfaces are available in reference 3 and cases not specifically calculated may be determined by interpolation of these results.

The contribution of the constant-load sectors used to form the trailing edge may be calculated in accordance with the methods presented in reference 2. This part of the solution presupposes a knowledge of the spanwise distribution of lifting pressure to be canceled. For a lifting triangle of infinite chord with subsonic leading edges, the lifting pressure along the leading edge is theoretically infinite. In the application of the method suggested in reference 2 for calculating the contribution of the canceling solutions to the downwash distribution, it is convenient to make some simplifying assumption regarding the magnitude of the lifting pressure along the extension of the leading-edge line. However, any assumption concerning the load distribution will, of course, affect the downwash. Hence a study was made to determine the effect of varying the assumption of the magnitude of the lifting pressure along the extension of the leading-edge line. For convenience, this pressure was expressed in terms of the lifting pressure along the center line of the lifting surface. The value of this ratio $\left(\frac{\text{leading-edge lifting pressure}}{\text{center-line lifting pressure}}\right)$ was varied between 5 and 50. It was found that increasing the value of the ratio beyond 10 yielded increments in $(d\epsilon/d\alpha)_{\alpha=0}$ which

were so small that they were masked by random errors in the mechanical integration involved in the calculations. Therefore, in the subsequent computations, the lifting pressure along the extension of the leading edge was assumed to be 10 times as great as that at the center line. The theoretical values of $(d\epsilon/d\alpha)_{\alpha=0}$ presented are therefore not influenced by the limitations imposed on the lifting pressure in the canceling solutions.

Effect of Displacement of the Vortex Sheet on the Downwash

All of the methods now available for computing downwash in supersonic flow are based on solutions of a linearized differential equation and are subject to the usual limitations of this simplified theory. The boundary conditions are satisfied in the $z=0$ plane (i.e., the plane of the wing) and the assumption is made that the free-stream direction coincides with that of the positive x axis. Thus, under these conditions, the trailing vortex sheet is assumed to be in the plane of the wing and to extend unchanged to infinity; this assumption also applies in subsonic thin-airfoil theory. Experimental results in subsonic flow have shown that this assumption does not adequately describe the flow field behind a lifting surface except at very small angles of attack. It has been shown (reference 4) that at finite angles of attack the vortex sheet is displaced from the plane of the wing due to the action of the downwash itself, and that the shed vorticity tends to concentrate into two vortices resulting in a rolling up of the vortex sheet. In calculating the downwash for conventional wing-tail combinations in subsonic flow, it has been found necessary to account for the movement of the vortex sheet and the resultant effects on the downwash distribution. However, the rolling up of the vortex sheet has been neglected because with high-aspect-ratio wings and normal tail locations the tail is not in the region affected.

In the application of the methods presented in reference 2 to compute the downwash at supersonic speeds, it is assumed that the shed vortex sheet coincides with the extended chord plane of the wing. Thus, in the calculations, the vertical location of any point in the flow field is taken from its position relative to the extended chord plane. However, in the actual flow under lifting conditions when the vortex sheet is displaced from the chord plane, the effective vertical location of any point in the flow field is different from that assumed in the linear theory. (The effective vertical location may be defined as the distance between the vortex sheet and the point in question.) The displacement of the vortex sheet is a function of the downwash

which is in turn dependent on the angle of attack of the lifting surface. Thus, although a point in the flow field may be fixed relative to the lifting surface, the effective vertical location will vary with the angle of attack. Since the linear theory shows that the downwash varies with distance above or below the vortex sheet, being a maximum at the vortex sheet and zero on the Mach cone, it is apparent that the rate of change of downwash angle with angle of attack at a point in the stream which is fixed relative to the lifting surface will vary as the angle of attack is changed.

An approximation to the effect of the displacement of the vortex sheet on the downwash, may be calculated by means of the linear theory in a manner similar to that employed in reference 4 and considered in more detail in reference 1. In the present report this approach has been used to compute the theoretical downwash angles through the angle-of-attack range at all survey points inboard of the wing tip. Since the theoretical approach used in this analysis cannot be used to calculate downwash near the extended leading-edge line, the computation of the flow-field deformation outboard of the wing tip was not undertaken. However, the values of $d\epsilon/d\alpha$ at $\alpha=0$ have been computed for the survey points which were outboard of the tip.

RESULTS

The spanwise distribution of the experimentally measured local stream angles are presented in figure 3. For clarity in presentation, these stream angles are plotted as $\alpha-\epsilon'$. These experimental results have also been plotted in figure 4 to show the variation of downwash angle ϵ' with angle of attack α at each survey point. Theoretical curves obtained as described in the preceding section are included for each case in which they were calculated. The slopes at $\alpha=0$ obtained from experimental plots similar to those presented in figure 4 are summarized in figure 5 along with the values of $(d\epsilon/d\alpha)_{\alpha=0}$ calculated in accordance with the methods of references 2 and 3.

In figure 6, wake profiles showing both the pitot-pressure loss in the viscous wake and the vertical position of the wake are presented for two streamwise positions at $\alpha=3^{\circ}$. In order to show the position of the upper limit of the friction wake relative to the extended chord plane, spanwise plots of the position of the upper limit of the wake at several angles of attack at survey stations 5 and 6 are shown in figure 7. From the same tests the position and movement of the wake center line were determined. In figure 8 these

results are compared to the movement predicted on the basis of linear theory.

DISCUSSION

Spanwise Variation of the Induced Stream Angle

In order to indicate the nature of the downwash field induced by the triangular lifting surface, the results of the surveys have been plotted in figure 3 to show the spanwise variation of induced stream angle at the three survey stations for several angles of attack. These results show that with the wing at negative angles of attack there are no abrupt changes in the induced stream angle over the extent of the spanwise surveys at any of the survey stations. This condition also prevails at small positive angles of attack. However, with the wing at approximately 2.5° angle of attack or greater the spanwise distributions exhibit irregularities involving abrupt changes in the induced stream angle of as great as 26° (station 2, α=10°). The spanwise distributions of stream angle at station 2 for α=10° and at station 4 for α=5° immediately suggest the presence of a vortex, the core of which was approximately in the stream direction. The direction of flow in the vortex was similar to that of a wing-tip vortex wherein the flow is around the wing tip from the high-pressure side to the low-pressure side. As the angle of attack was increased, the data indicate that the vortex core moved toward the wing root.

It might be expected that the formation of such a vortex would accompany a change in the span loading with increasing angle of attack. Low-speed pressure-distribution tests (references 5 and 6) of similar triangular wings showed an inboard shift of the center of pressure with increasing lift. Visual observation of these tests detected the presence of vapor trails, believed to be vortex cores, originating near the leading apex and passing over the low-pressure surface inboard of the wing tips. The path of these trails was coincident with pressure peaks in the chordwise pressure distributions and the occurrence of these trails was associated with leading-edge separation and center-of-lift movement. Successive improvements of the leading-edge profile involving rounding of the leading edge, use of an NACA 0012 section, and use of an NACA 65-series low-drag section resulted in elimination of the condensation phenomenon altogether, a reduction in the magnitude of the pressure peaks, and a delay in the inboard movement of the center of lift to higher angles of attack. Pressure-distribution tests at M=1.53 (reference 7) of a wing with the same leading-edge sweep angle as the triangular wing

used in this downwash investigation, however, did not indicate the variations in loading which might be anticipated. The probable reason for this lies in the large difference in the leading-edge profiles of the two wings. Although the leading edges of both wings were sharp, the pressure-distribution model had a biconvex airfoil section with a leading-edge wedge angle of 36° measured normal to the leading edge; whereas the wedge angle for the double-wedge section of the triangular plan-form wing was only 12-1/2°.

Schlieren photographs and liquid-film tests presented in reference 8 for a triangular plan-form wing of aspect ratio 0.7 at M=1.62 indicate the presence, in the induced flow field, of vortices similar to those detected in the present tests. Under lifting conditions two distinct line vortices appear behind the trailing edge inboard of either tip. The liquid-film tests show that on the wing the outer lines of vorticity coincide approximately with the ridge line.

The results of the stream-angle measurements shown in figure 3 indicate that, if this wing were to be used as a forward lifting surface in a tandem arrangement of lifting surfaces, severe interference effects on the trailing surface might be expected if the trailing surface were located in a position similar to station 2 or 4.

Rate of Change of Downwash at Zero Lift

The theoretical values of $(d\epsilon/d\alpha)_{\alpha=0}$ used for comparison with the experimental results in figure 5 were obtained from the charts of reference 3 and the method of calculation outlined in reference 2. The experimental values of $(d\epsilon/d\alpha)_{\alpha=0}$ were taken from the curves of figure 4 and represent the slope at $\alpha=0°$ of curves faired through the experimental points. These summary plots show that the experimental trends of increasing $(d\epsilon/d\alpha)_{\alpha=0}$ as the plane of the wing is approached and, as the distance downstream from the wing is increased, are consistent with the theoretical predictions. The agreement between the experimental and theoretical spanwise variation of $(d\epsilon/d\alpha)_{\alpha=0}$ is good inboard of approximately the 70-percent-semispan position. The agreement in the remainder of the field outboard of this position is not as good. It appears that the upwash field has been shifted somewhat inboard from the position predicted by the linear theory.

Variation of Downwash With Angle of Attack

For convenience in considering the variation of the downwash

angle with angle of attack, the following discussion is divided into two sections. The first will be concerned with the region for which the theory predicts positive values of $(d\epsilon/d\alpha)_{\alpha=0}$ which corresponds to a region of downwash for positive angles of attack. The second is that part of the induced flow field for which the theory predicts upwash at positive angles of attack. For each of the survey stations the theory predicts downwash from the wing root (vertical plane of symmetry) out to approximately the 86-percent-semispan station; the balance of the survey points are in the region of theoretical upwash.

Downwash region.- The calculations which have been performed for each of the survey points within the downwash region show that the slope of the curve defining the theoretical variation of the downwash angle ϵ', with the angle of attack α, increases as the angle of attack is increased from -10° to $+10^\circ$. (See fig. 4.) This same trend is followed by the experimental results; however, the rate of increase of the slope is usually larger than predicted; at negative angles of attack the slopes are less; and at positive angles of attack the slopes are generally greater. This departure from the predicted values is believed to result from two factors.

The more important of these two factors is believed to be the existence of the strong vortex which is not predicted by the linear theory. The effect of this vortex at each of the survey positions will, of course, depend on its strength as well as its position relative to the survey point. The results of the surveys indicate that the strength of the vortex increased as the incidence of the wing was increased in either the positive or negative range and that the vortex core always originated on the low-pressure surface of the airfoil. Thus, since the survey positions were above the extended chord plane of the wing, the effect of the vortex on the downwash at each point was greatest in the positive angle-of-attack range and increased with increasing angle of attack.

The data in the positive angle-of-attack range at station 2 illustrate most clearly the effect of the vortex on the downwash distribution. At the 14-percent-semispan position the downwash angle increased much more rapidly with increasing angle of attack than predicted by theory. This same trend is continued at each survey position out to and including the 57-percent-semispan position. The agreement between the experiment and theory deteriorates as this latter survey position is approached. This results primarily from the fact that each successive survey position is closer to the vortex core and thus the vortex affects the downwash to a greater degree. At the 71- and 86-percent-semispan positions, the experimental results at $\alpha=5^\circ$ were very similar to those for the other inboard

positions in that the measured downwash angles were much larger than the values predicted by theory. However, at each of these positions the flow changed from downwash to upwash when the angle of attack of the wing was increased from 5° to 10°. This was apparently the result of the inboard movement of the vortex core. The data in figure 3 indicate that for $\alpha=5^\circ$ the vortex core was between the 86- and 100-percent-semispan positions; whereas at $\alpha=10^\circ$ it had moved inboard and was between the 57- and 71-percent-semispan positions. Thus at $\alpha=5^\circ$, both the 71- and 86-percent-semispan survey positions were inboard of the vortex core and hence in its downwash field; at $\alpha=10^\circ$, the vortex had moved inboard so that the survey positions were in the upwash field of the vortex. Although the examples used have been confined to the data obtained at station 2, the analysis is equally applicable to the data for the other survey stations if proper consideration is given to their positions relative to the vortex.

In considering the variation of ϵ' with α in the negative angle-of-attack range, it might be anticipated that the vortex would have little effect on the perturbation velocities at any of the survey points since in this range the vortex was distant from the survey points, being, in fact, on the opposite side of the extended-chord plane. Nevertheless, since the presence of the vortex in the flow field resulted in downwash angles which were greater than the theoretical at moderate positive angles of attack, its presence should produce upwash angles greater than the theoretical at negative angles of attack. However, it is apparent from the plots in figure 4 that the measured upwash angles at the survey points were generally less than those predicted by theory. Hence, it must be concluded that the effect of the vortex on the perturbation velocities at the survey points is small in the negative angle-of-attack range and is in fact overshadowed by a second factor which may contribute to the departure of the experimental results from the theoretical predictions at finite angles of attack. The vortex sheet, or what is equivalent, the center line of the wake, was not displaced from the free-stream direction as far as calculated. (See fig. 8.) Therefore, with the wing at positive angles of attack, the points at which the downwash angles were measured were actually much closer to the point of maximum downwash at the wake center line than the theory predicts. Since, in accordance with theoretical considerations, the downwash increases with decreasing distance from the vortex sheet, it is apparent that the actual downwash at the survey points would be greater than predicted. Conversely, in the negative angle-of-attack range this effect was reversed, that is, the survey points were farther from the vortex sheet than the theory predicts; thus the actual upwash was less than the theoretical.

[redacted]

In both the positive and negative angle-of-attack ranges, a combination of the two effects discussed is measured and, since the magnitude of neither is known, any quantitative evaluation of these effects is precluded. It is apparent from the data at the 71- and 86-percent-semispan positions at station 2, and the 71-percent-semispan position at station 4, however, that the vortex had the greater effect. The abrupt decrease in downwash which occurred in the positive angle-of-attack range can only be attributed to the effect of the vortex since, if only the displacement of the vortex sheet were considered, it would be expected that the slope of the curves of the variation of ϵ with α would continue to increase up to the maximum angle of attack of these tests.

Upwash region.- In the region in which negative values of $d\epsilon/d\alpha$ at $\alpha=0$ are predicted, the theoretical calculations were limited to the evaluation of the rate of change of downwash angle at zero lift. The straight lines representing these values have been extended for approximately $\pm 4^{\circ}$ around $\alpha=0$ for comparison with the experimental results. The rapid increase in upwash with increasing angle of attack which occurred at the 100-percent-semispan position at all three of the survey stations may have resulted from either the self-induced distortion of the flow field outboard of the wing tip or from the vortex in the flow field behind the wing. The experimental results indicate that at stations 2 and 3, the upwash region extended somewhat inboard of the theoretical boundary.

Wake

The pitot-pressure profiles presented in figure 6 indicate the location, thickness, and intensity of the wake for several semispan positions at survey stations 5 and 6 which were 1.79 and 2.34 root-chord lengths aft of the leading apex, respectively. The horizontal reference line used in this figure is a line drawn in the free-stream direction through the apex of the wing. The general characteristics of the wake are similar to those observed in subsonic flow in that, with increasing distance downstream from the wing, the wake expanded slowly, decreased in intensity, and, with the wing at positive angles of attack, moved downward relative to the free-stream reference line. As can be seen from this plot the pitot-pressure profiles are similar to those of the dynamic-pressure variation through the friction wake behind a lifting surface in subsonic flow. The intensity of the wake, as reflected by the maximum pitot-pressure loss, was largest behind the wing root and decreased to a minimum behind the wing tip. The data indicate that, for the four outboard survey positions, the maximum pitot-pressure loss decreased almost linearly toward the

minimum behind the wing tip; however, the maximum loss behind the 14-percent-semispan station appears to be disproportionately large. Since this survey station was relatively close to the boundary-layer plate, it is believed that this large pitot-pressure loss is not representative of conditions for the wing alone but rather results from interference between the model and support. A similar condition was observed in connection with the wake surveys made for the rectangular plan-form wing reported in reference 1.

It should be pointed out that the large maximum pitot-pressure loss measured at the 14-percent-semispan position indicates that, even though the stream velocity at the wake center line may have been supersonic, it is possible that the Mach number was sufficiently low to allow interference between adjacent tubes in the survey rake. Therefore, near the wake center line at the 14-percent-semispan position, the pitot pressures indicated by the tubes in the rake may be slightly different from what would have been obtained if a single isolated tube had been used for the survey.

To show the large region behind the wing in which the viscous effects may be important, the position of the upper limit of the wake at stations 5 and 6 for several angles of attack is shown in figure 7. Only the upper limit of the wake is shown since the wake thickness is essentially independent of angle of attack for this range and the half thickness is defined at $\alpha=0^\circ$.

The position of the wake center line relative to the extended-chord plane of the wing has been determined and compared in figure 8 to the position calculated by means of the linear theory. Although the wake center line is somewhat farther above the chord plane than the theory predicts, over the inboard 50 percent of the semispan the incremental movement of the center line between $\alpha=3^\circ$ and 6°, and between 6° and 9°, corresponds quite closely to that predicted by the theory. The high position of the wake at $\alpha=3^\circ$, 6°, and 9° at the outboard stations indicates the vortex sheet is rolling up and infers that, in this region, the downwash at the wake center line is not as great as predicted by linear theory.

CONCLUDING REMARKS

The results obtained in this investigation show that the linear theory is suitable for determining $d\epsilon/d\alpha$ at $\alpha=0$ within that portion of the induced flow field for which the theory predicts positive values of $(d\epsilon/d\alpha)_{\alpha=0}$.

[redacted]

The downwash surveys show that under lifting conditions there is a strong vortex in the induced flow field of the triangular planform wing used in this investigation. The vortex has considerable effect on the downwash distribution and thus on the position of the shed vortex sheet at finite angles of attack. These effects are so large in the positive angle-of-attack range that predictions of the downwash angles based on the linear theory are of little value at any but small angles of attack. If this wing were to be used as a forward lifting surface in a tandem arrangement of lifting surfaces, the possibility of severe interference effects on the trailing surface should be investigated. The rather large variations in the rate of change of downwash angle with angle of attack which occur at the higher angles of attack might result in nonlinear pitching-moment characteristics.

Ames Aeronautical Laboratory,
National Advisory Committee for Aeronautics,
Moffett Field, Calif.

REFERENCES

1. Perkins, Edward W., and Canning, Thomas N.: Investigation of Downwash and Wake Characteristics at a Mach Number of 1.53. I – Rectangular Wing. NACA RM No. A8L16, 1948.

2. Lagerstrom, P. A., and Graham, Martha E.: Downwash and Sidewash Induced by Three-Dimensional Lifting Wings in Supersonic Flow. Douglas Aircraft Co., Inc., Rep. No. SM-13007, Apr. 1947.

3. Nielsen, Jack N., and Perkins, Edward W.: Charts for the Conical Part of the Downwash Field of Swept Wings at Supersonic Speeds. NACA TN No. 1780, 1948.

4. Silverstein, Abe, Katzoff, S., and Bullivant, W. Kenneth: Downwash and Wake Behind Plain and Flapped Airfoils. NACA Rep. No. 651, 1939.

5. Anderson, Adrien E.: Chordwise and Spanwise Loadings Measured at Low Speed on Large Triangular Wings. NACA RM No. A9B17, 1949.

6. Wick, Bradford H.: Chordwise and Spanwise Loading Measured at Low Speed on a Triangular Wing Having an Aspect Ratio of 2 and an NACA 0012 Airfoil Section. NACA TN No. 1650, 1948.

[redacted]

7. Boyd, John W., Katzen, Elliot D., and Frick, Charles W.: Investigation at Supersonic Speed (M=1.53) of the Pressure Distribution Over a 63° Swept Airfoil of Biconvex Section at Several Angles of Attack. NACA RM No. A8F22, 1948.

8. Love, Eugene S.: Investigations at Supersonic Speeds of Twenty-Two Triangular Wings Representing Two Airfoil Sections for Each of Eleven Apex Angles. NACA RM No. L9D07, 1949.

[redacted]

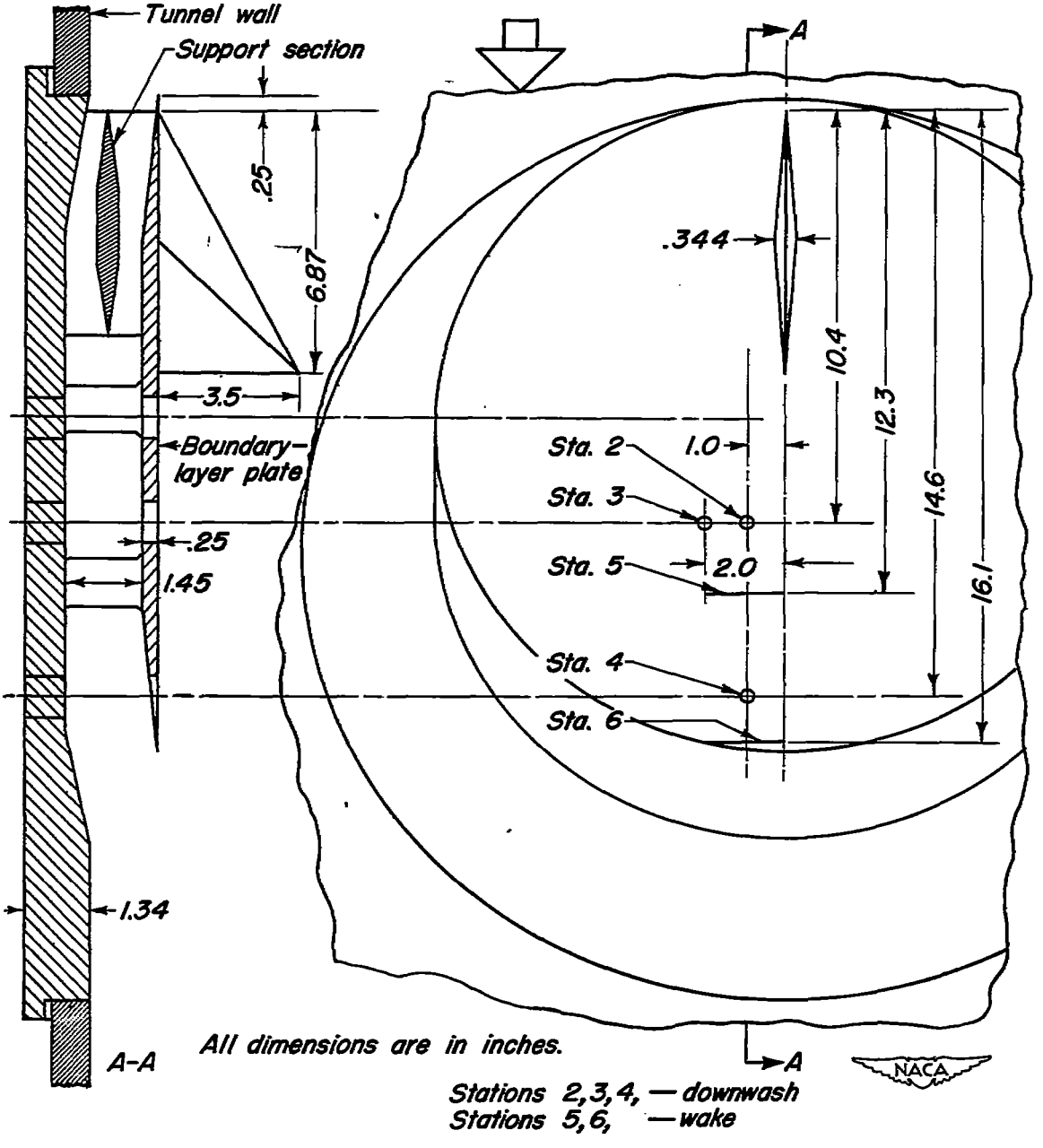

Figure 1. — Sketch of model support system showing location of survey stations.

[redacted]

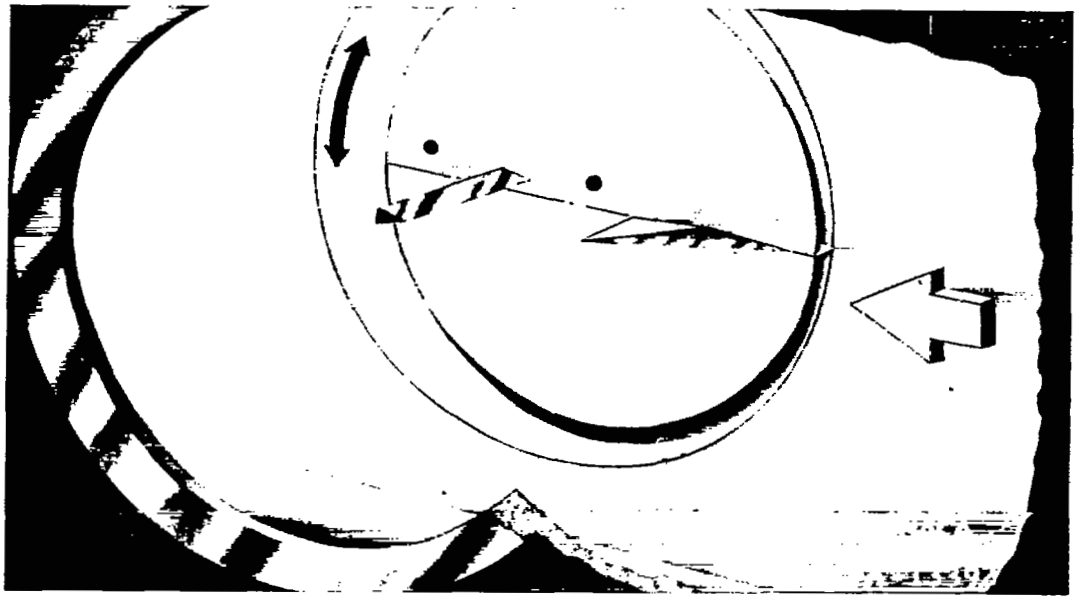

(a) Semispan model of the triangular wing with the stream-angle wedge. $\alpha = 0^\circ$

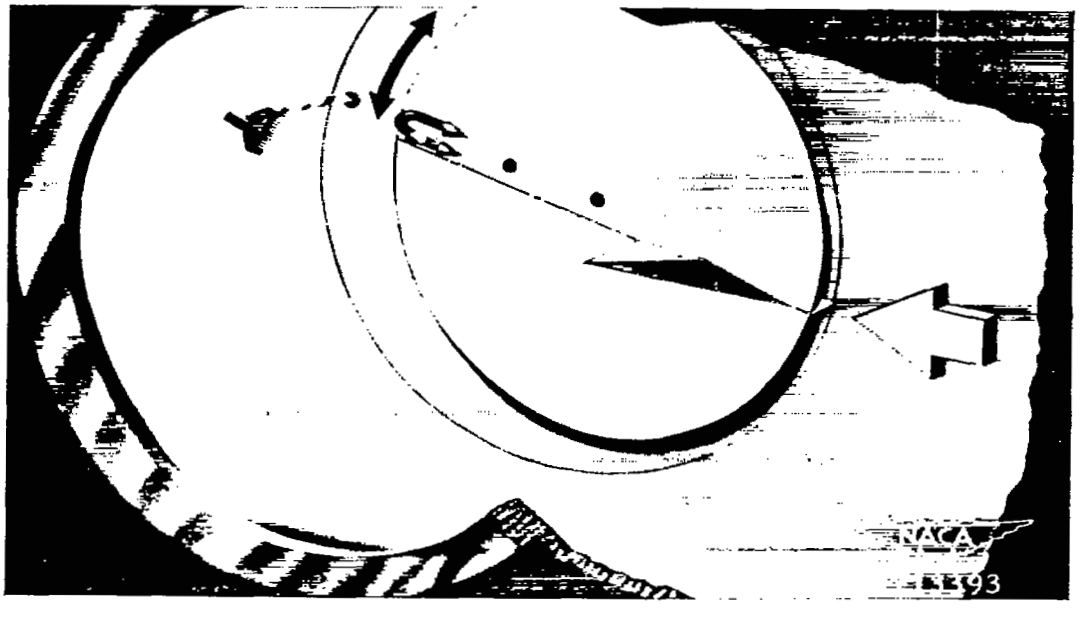

(b) Semispan model of triangular wing with stream-angle cones and wake survey rake. $\alpha \cong -10^\circ$

Figure 2.– Sketch of the test section showing the boundary-layer plate, the semispan model, and the survey instruments.

[redacted]

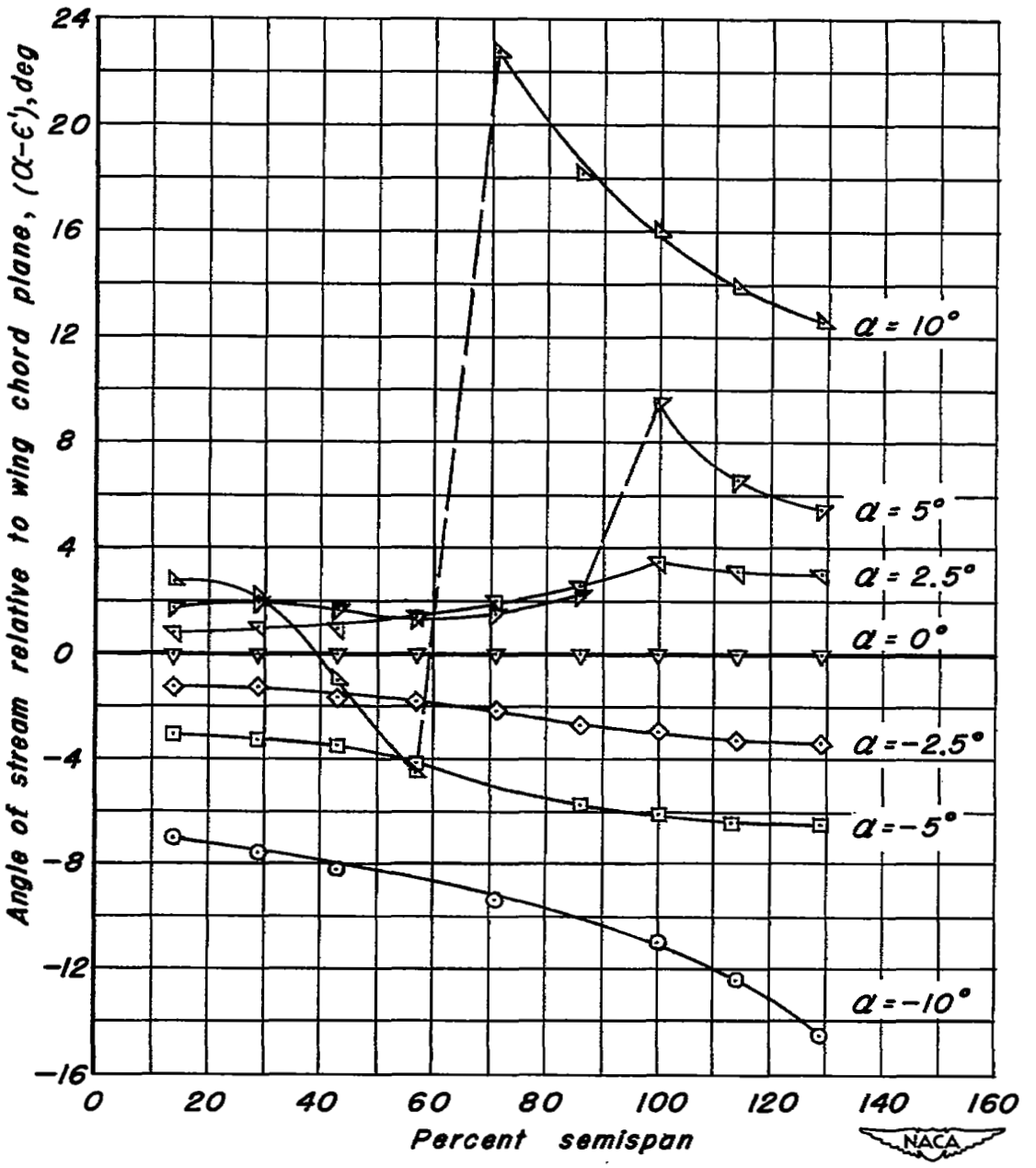

(a) Station 2, $x = 1.52\ c$, $z = 0.146\ c$.

Figure 3.— Spanwise variation of stream angle behind a triangular lifting surface.

[redacted]

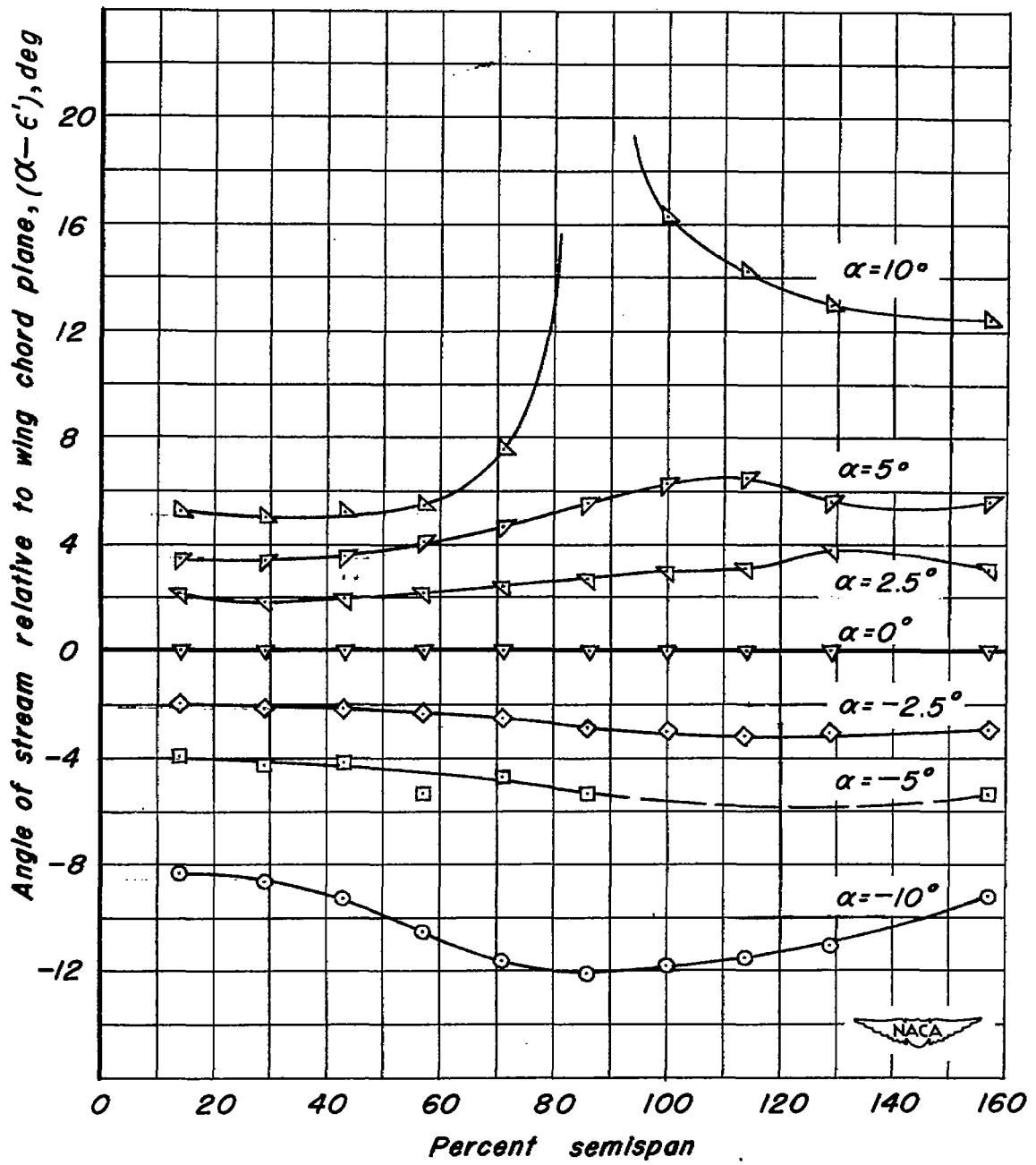

(b) Station 3, $x = 1.52\ c$, $z = 0.29\ c$.

Figure 3.— Continued.

[redacted]

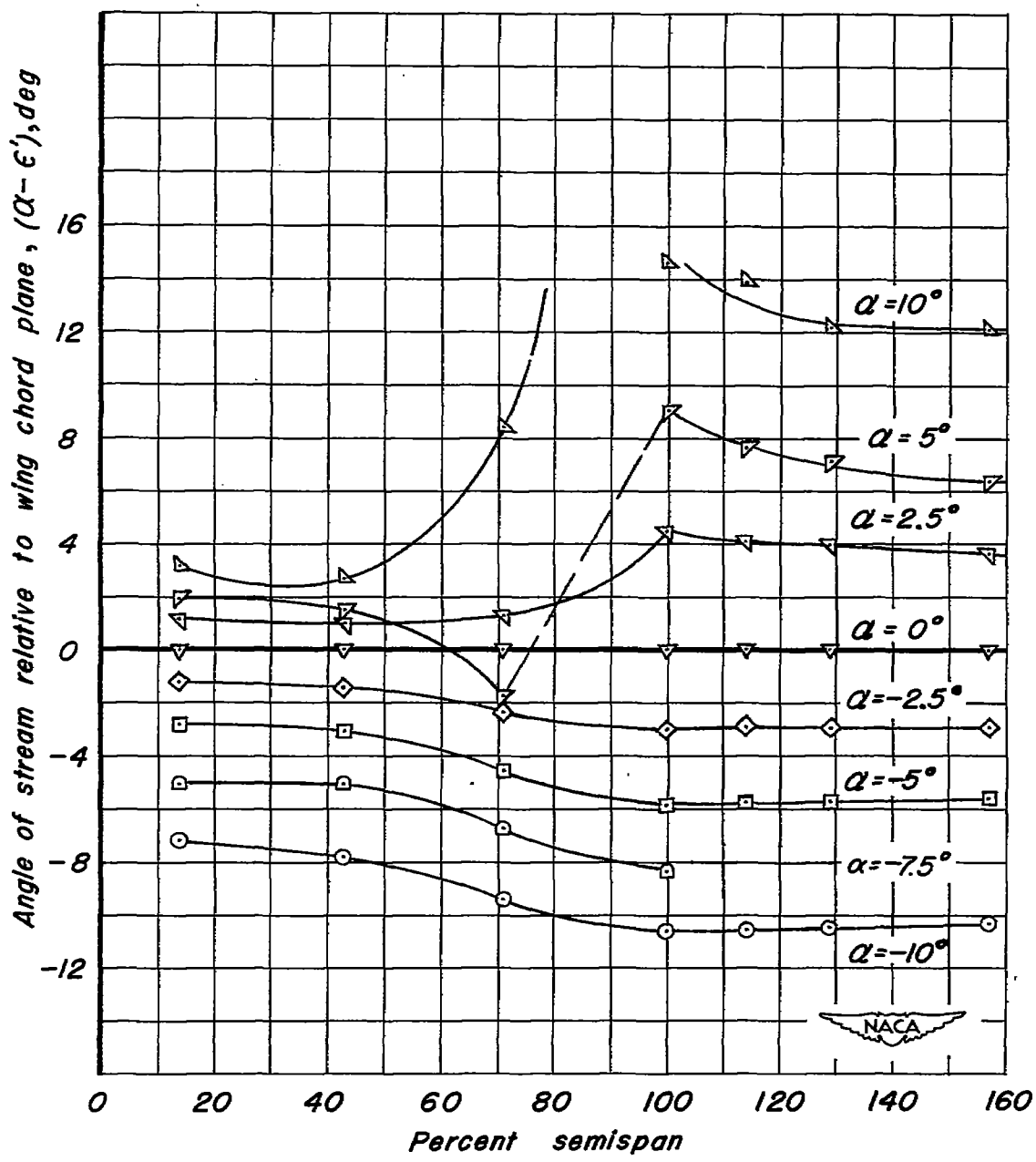

(c) Station 4, x = 2.12 c, z = 0.146 c.

Figure 3. — Concluded.

[redacted]

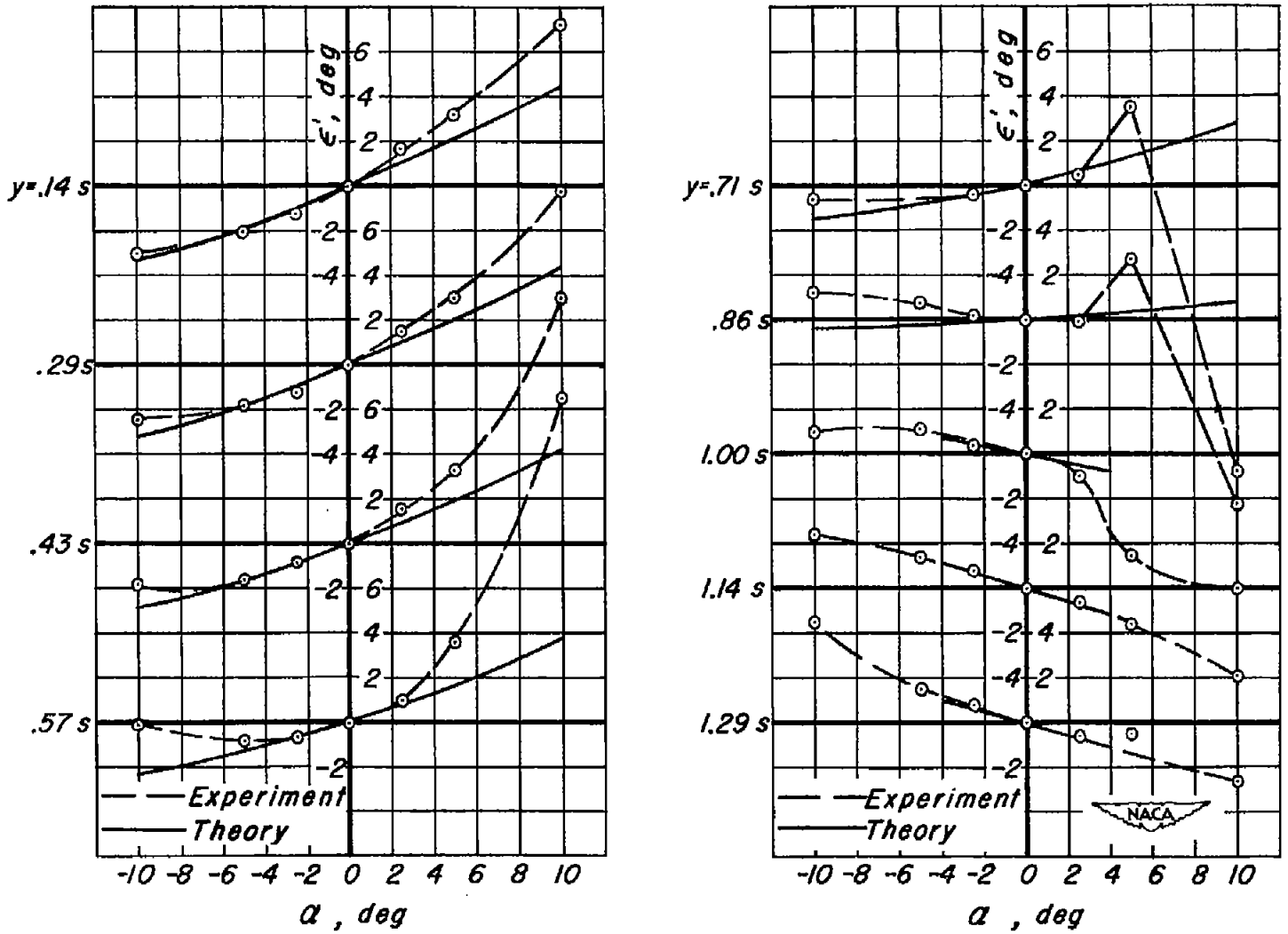

(a) Station 2, x=1.52 c, z=0.146 c.

Figure 4.— Variation of downwash angle with angle of attack.

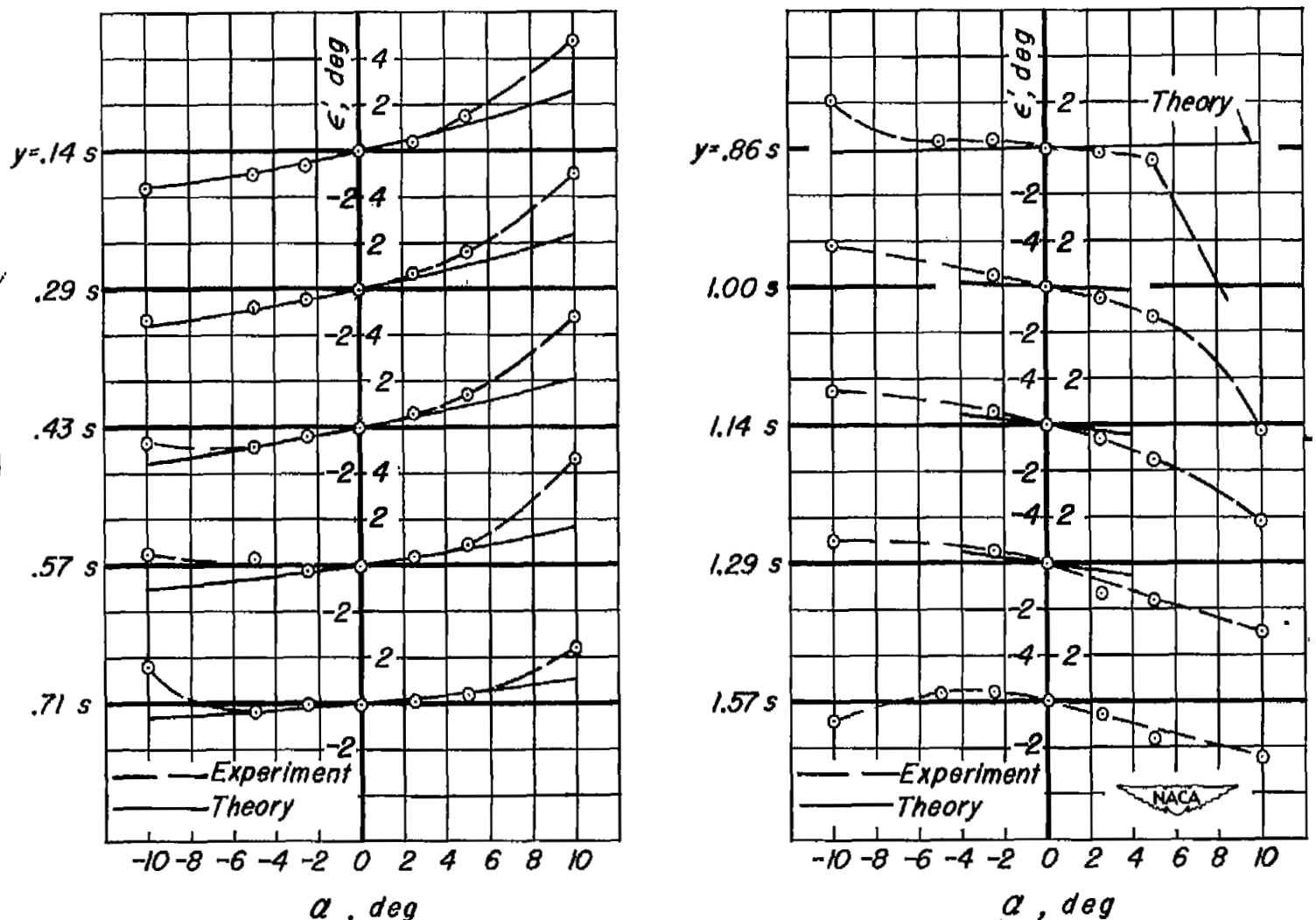

(b) Station 3, $x = 1.52\,c$, $z = 0.29\,c$.

Figure 4. — Continued.

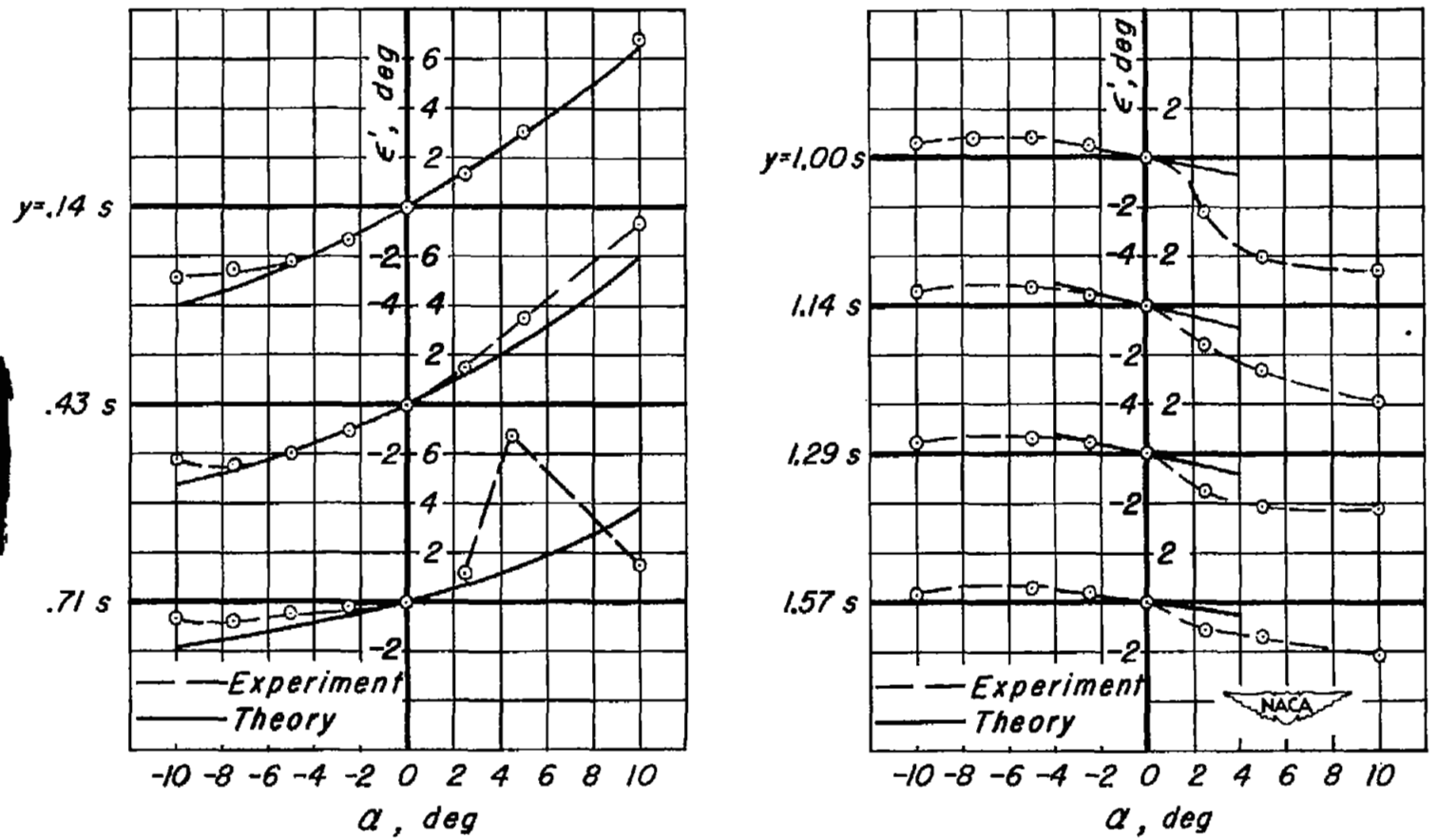

(c) Station 4, x=2.12 c, z=0.146 c.

Figure 4.— Concluded.

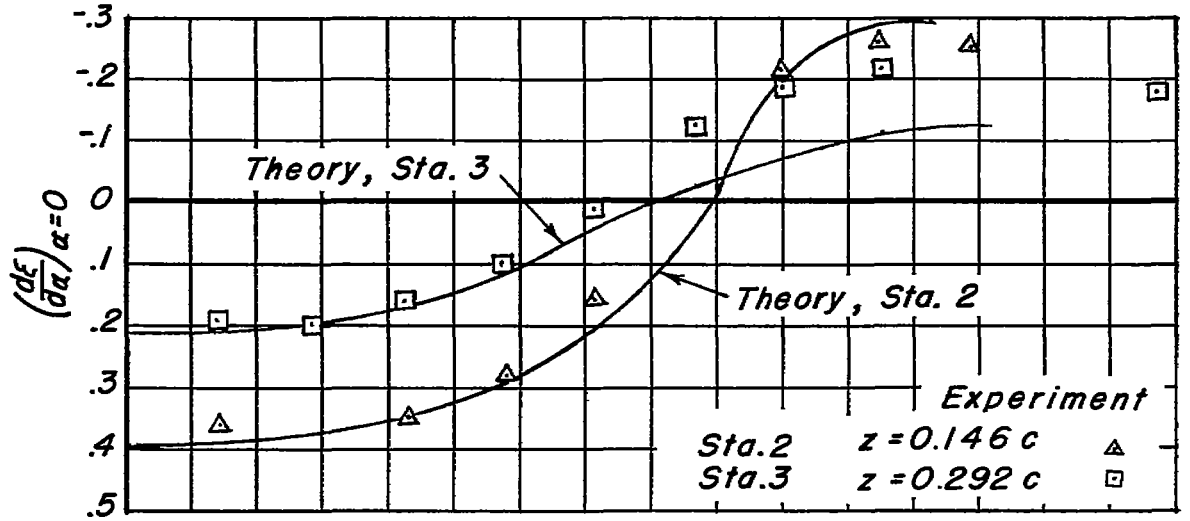

(a) x=1.52c.

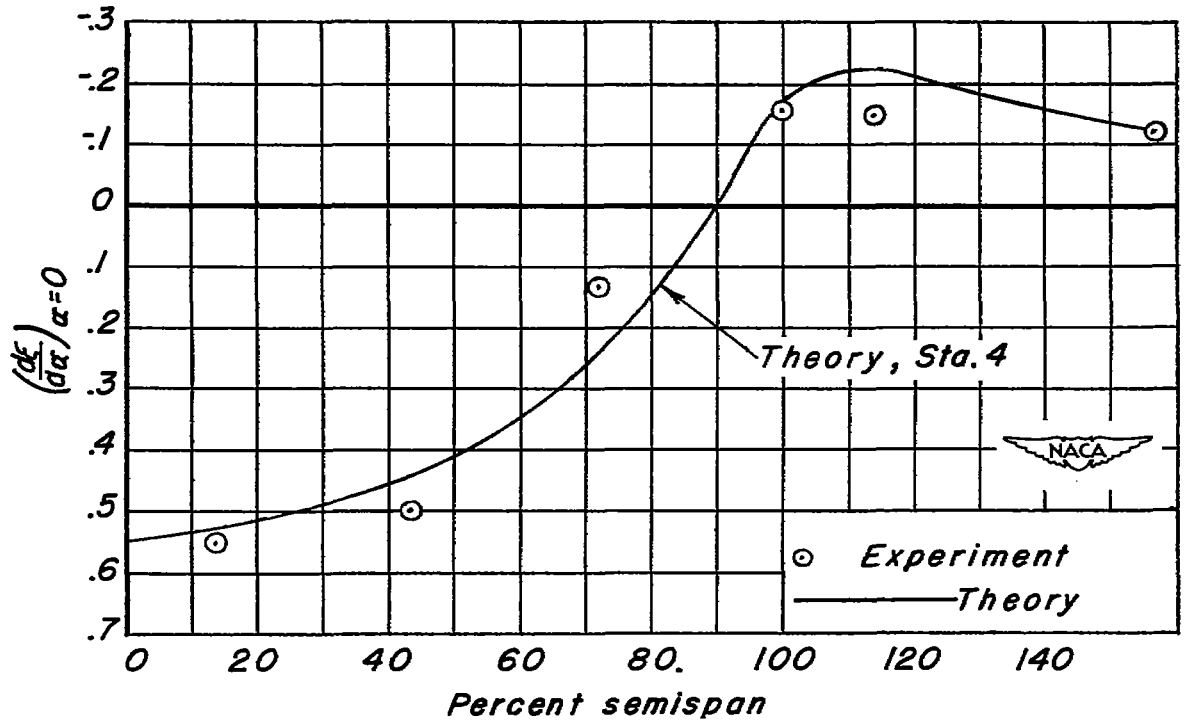

(b) Sta.4, x=2.12c, z=0.146c.

Figure 5.—Spanwise variation of $\left(\frac{d\varepsilon}{d\alpha}\right)_{\alpha=0}$ behind triangular wing.

[redacted]

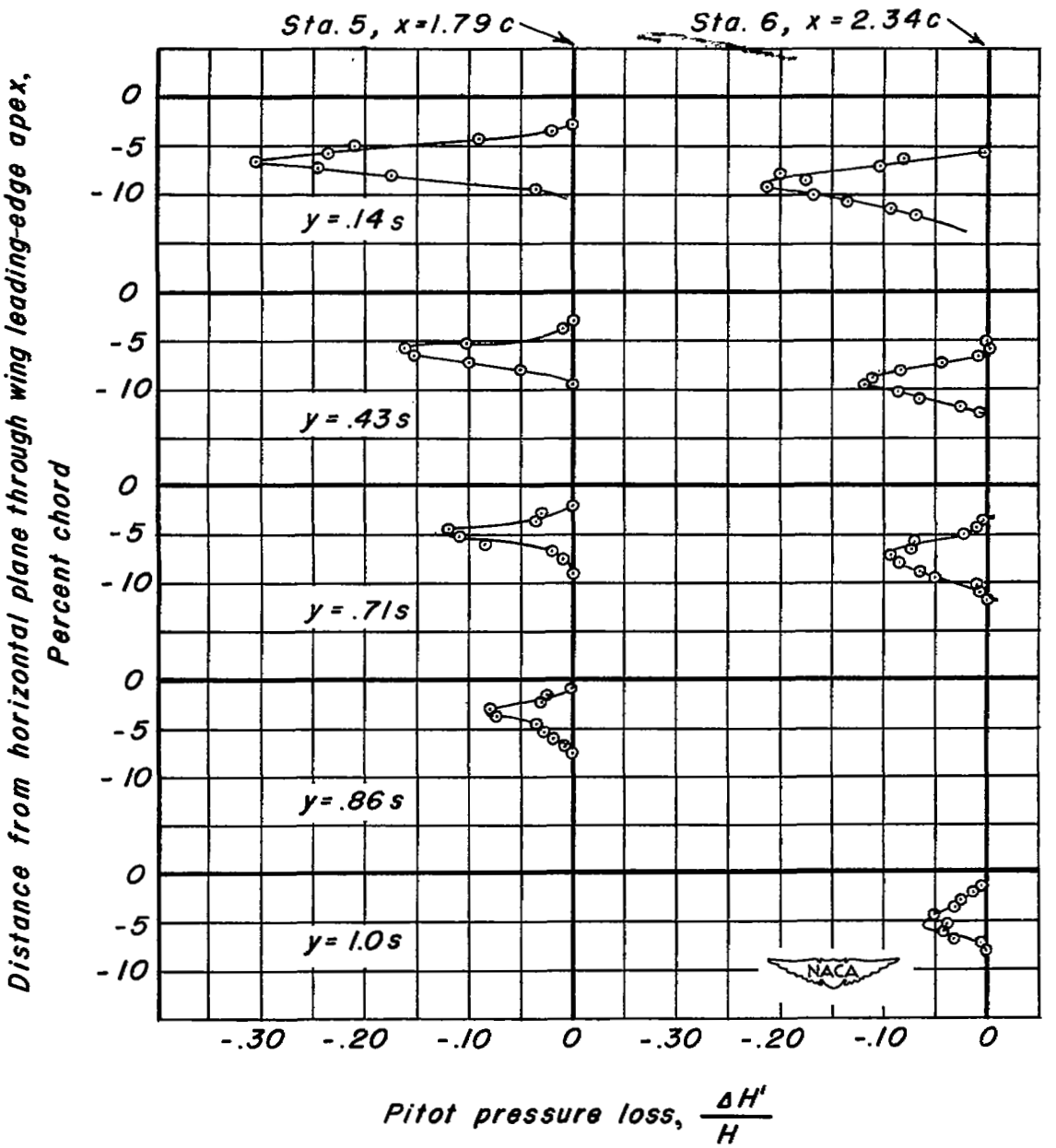

Figure 6.—Profiles of pitot pressure loss through viscous wake of triangular wing; $\alpha = 3°$.

[redacted]

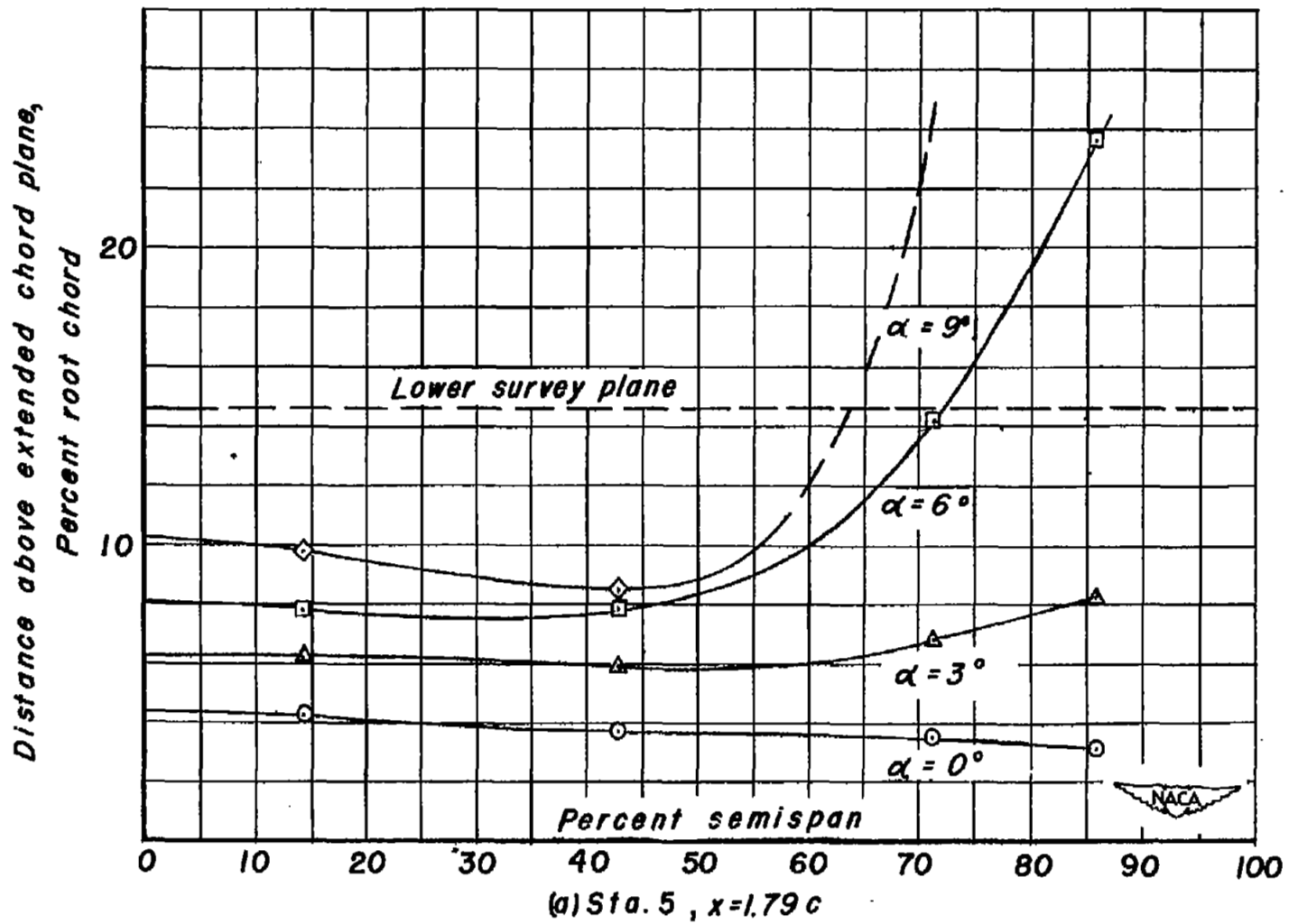

Figure 7 .—Position of upper limit of the viscous wake relative to extended wing chord plane.

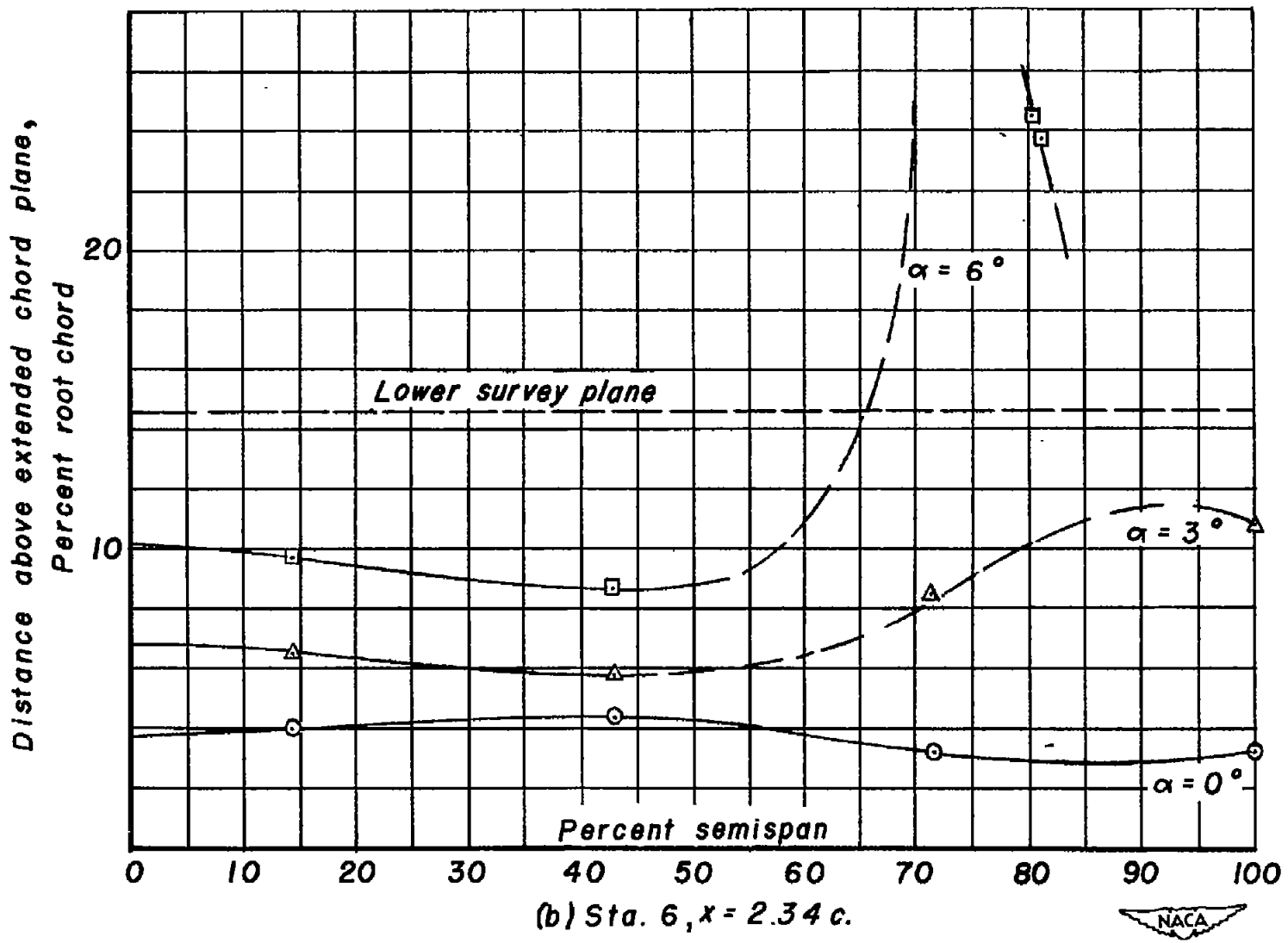

Figure 7 .—Concluded.

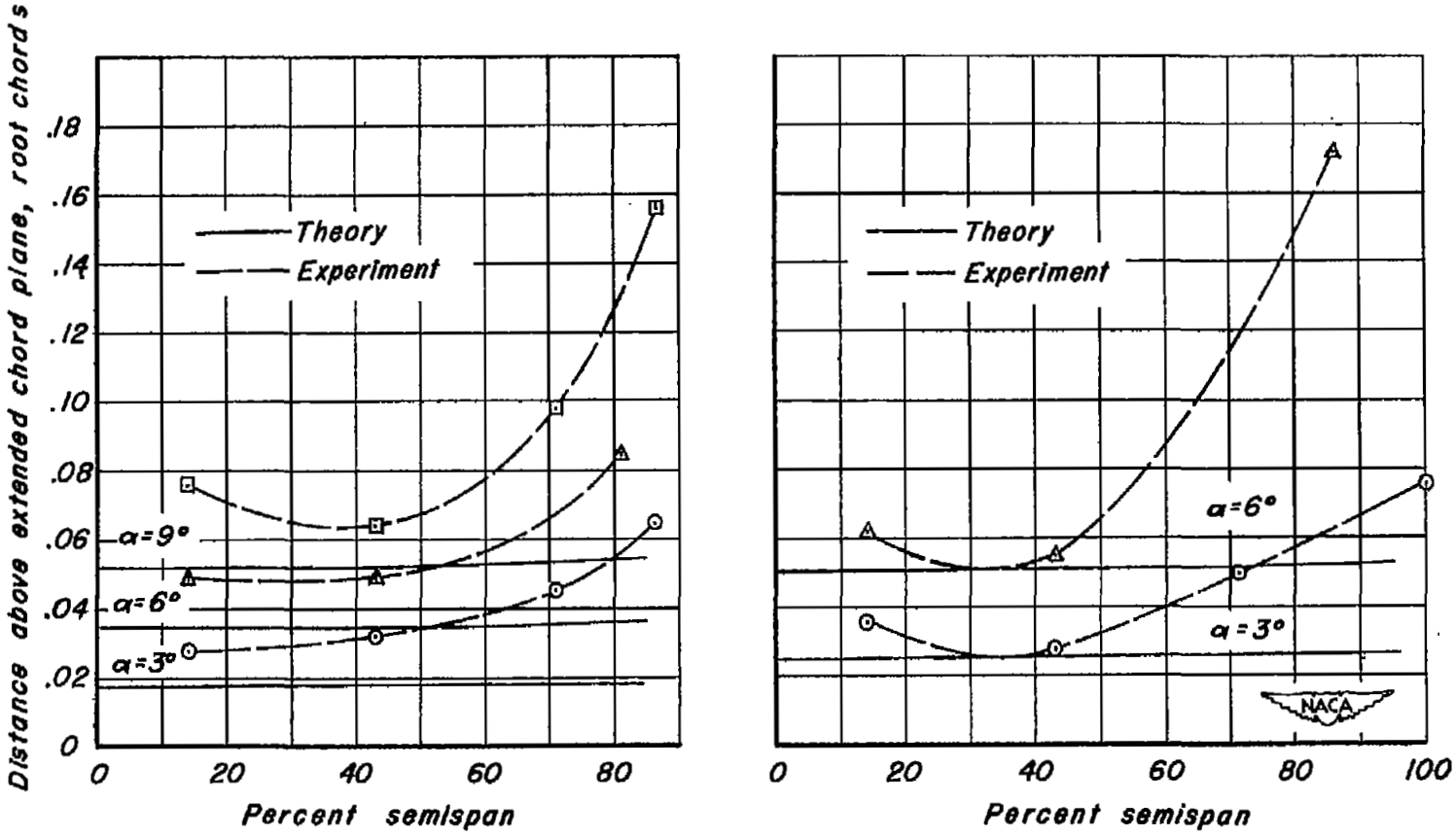

Figure 8.— Position of the centerline of the viscous wake relative to extended wing chord plane.